Mechanical Properties of the 2D Re-entrant Honeycomb Made via Direct Metal Printing

Amer Alomarah[12], Jianjun Zhang[1], Dong Ruan[1]*, Syed Masood[1] and Guoxing Lu[1]

[1]Faculty of Science, Engineering and Technology, Swinburne University of Technology, Hawthorn, VIC 3122, Australia
[2]Department of Mechanics, College of Engineering, Wasit University, Al-Kut 52001, Iraq

* druna@swin.edu.au

Abstract. Auxetic structural materials show distinctive properties by exhibiting a negative Poisson's ratio (NPR). When these structures are subjected to uniaxial loading, they expand in tension and contract in compression in both loading and lateral directions. In this paper, two AlSi12 re-entrant honeycomb samples were manufactured using direct metal printing (DMP). Quasi-static uniaxial tension was executed in both X and Y direction. A Digital VIC-2D Image Correlation System was used to record the deformation history. Force and displacement were measured by ZWICK machine. The results show that loading direction has a significant effect on the mechanical properties and auxeticity of the tested structure. Re-entrant honeycomb under X-loading withstand lower force and has smaller magnitude of Poisson's ratio compared with that under Y-loading.

1. Introduction

Honeycombs evoke an extensive exploration because of their attractive mechanical properties represented with lightweight. These structures find dominant applications in different industries including automotive, aerospace, sports, marine and medical industries. Recently, developments in manufacturing technology have boosted the development of novel materials with remarkable performance to meet higher engineering specifications [1]. Unlike conventional materials, auxetic materials present uncommon geometric effect by becoming larger in all directions when stretched and smaller in all directions when compressed [2-4].]. Auxetic property tailors the structures to enhanced mechanical properties: indentation resistance, shear modulus, fracture toughness, variable permeability, and energy absorption [3-6]. Among many auxetic structural designs, re-entrant honeycomb has been studied extensively [7] due its intelligibility, adaptability and ability to produce high NPR which make it a favourable option for many applications [8, 9]. For re-entrant honeycomb, the key point to generate an auxetic behaviour is to select the proper unit cell dimensions and the re-entrant angles in the structure, which result in contraction of the structure in all directions under uniaxial compression, or expansion in all directions under uniaxial tension [10]. Additive Manufacturing (AM) or 3D Printing is becoming a more attractive technology for manufacturing of such structures because of its capability of not only providing geometric freedom but also offering precise control of micro-architecture and dimensions, thus turning any imaginable design into reality. Moreover, AM being a layer by layer building process, introduces its own influence on the performance and properties of the

fabricated structures due to anisotropy, build orientation and thermo-mechanical material behaviour during the building process. It is necessary to understand the behaviour of such additive manufactured metallic auxetic structures, especially if they are to be employed in NPR related applications. While there have been some studies on auxetic behaviour of titanium structures made by direct metal 3D printing processes such as electron beam melting (EBM) [11] and selective laser melting (SLM) [12], very little attention has been paid on auxetic behaviour of aluminium structures made by direct metal printing. The aluminium alloy AlSi12 is a favourable powder used in SLM metal printing process due to its good convergence between melting and solidification temperatures. The AlSi12 alloy is widely used in the applications that required superior thermal properties and lightweight such as automotive, aerospace and aviation. In this paper, powder of aluminium alloy (AlSi12) is used to manufacture two re-entrant honeycomb samples using SLM Direct Metal Printer technique. The large deformation behaviour of re-entrant honeycombs subjected to quasi-static tensile load is experimentally investigated. The mechanical properties and the effect of loading direction on the re-entrant honeycomb samples are reported.

2. Design and manufacturing of re-entrant honeycomb samples

In the current study, a unit cell of re-entrant honeycomb is described by five geometric parameters as shown in Figure 1 (a). H is the length of vertical walls, L is the length of inclined walls, θ is the re-entrant angle (the angle between vertical and inclined walls), t_1 is the cell wall thickness and t_2 (not shown) is the out-of-plane depth. The geometric parameters of the re-entrant unit cell are shown in table1. Figures 1 (b) and (c) present the re-entrant honeycomb samples. Moreover, five dog-bone samples in figure 1 (d) were also printed out using the same approach.

Aluminium Silicon Alloy (AlSi12) powder was used to fabricate two re-entrant honeycomb samples figure 1 (b) and (c). The average size of AlSi12 powder was 40 µm. The AlSi12 re-entrant honeycomb samples were manufactured using SLM Direct Metal Printing process based on the geometry model generated in CAD. The ProX200 direct metal printer was employed to build the re-entrant samples layer-by-layer by melting AlSi12 powders using 1.07 µm wavelength laser beam**.** The laser power and laser focal plane used were 240 W and 0.6 mm respectively. The travelling speed of laser beam was set to 2500 mm/sec. The total layers for each sample were 180 with an approximate thickness 40 µm for each layer. In order to eliminate the effect of building direction on the mechanical properties, both samples were manufactured in the same orientation the out-of-plane direction (depth). After printing re-entrant samples, wire cutting was used to separate the samples from the printing substrate, through CNC Wire cutting machine (Fanuc Robocut) model Alpha 0 C. Afterwards, both samples were coated with white and black paints to create a stochastic black and white spot pattern as required for the digital image correlation (DIC).

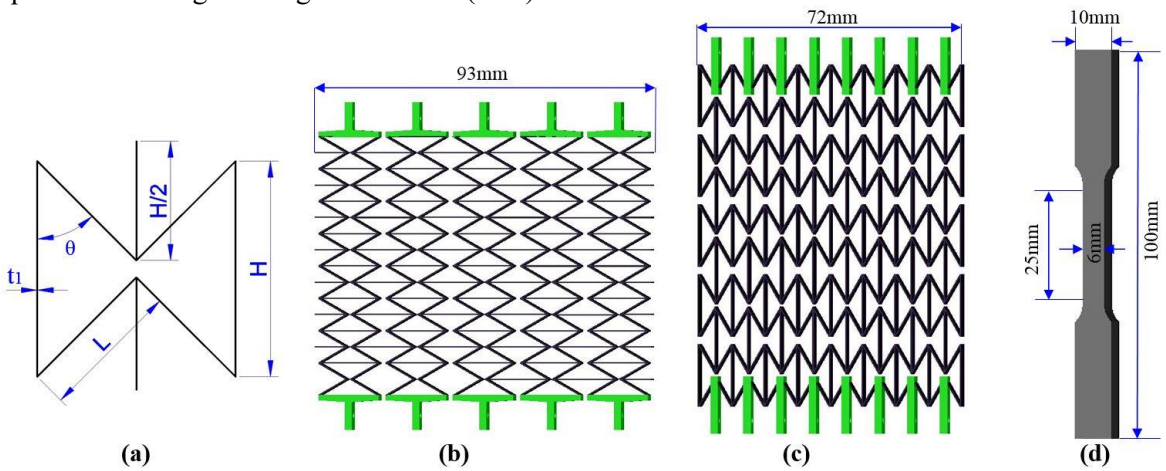

Figure 1. (a) A sketch of a unit cell of re-entrant honeycomb; (b) A re-entrant honeycomb under X-loading, (c) A re-entrant honeycomb under Y-loading, (d) A dog-bone sample used in tensile test to determine the material properties.

Table 1. Geometrical parameters of a unit re-entrant honeycomb cell.

structure	Material	H (mm)	L (mm)	θ (°)	t_1(mm)	t_2 (mm)
Re-entrant samples	AlSi12	16.8	8.4	30	0.36	7.2

3. Experimental setup

3.1 Tensile tests

In order to investigate the properties of the parent material of the re-entrant honeycomb, five tensile tests were firstly conducted on dog-bone samples and the stress-strain curves of these samples is shown in figure 2 (a). The cell wall material made of AlSi12 power is brittle, and the fracture strain is approximately 0.03. To overcome the restriction at both clamped ends during the tests, small stainless steel fixtures were manufactured to hold and grip the test sample at both ends, as in figure 2 (b). The spherical shape ends of these fixtures and lubricant used to reduce friction between contact surfaces. Tensile tests of auxetic samples were conducted using a Zwick Roell machine (Zwick/Z010) with a load cell of 1 kN. One sample was tensioned in the X direction figure 2 (c) and the other sample was tensioned in the Y direction figure 3 (a). The cross-head speed was 3 mm/min for both tests until fracture occurred.

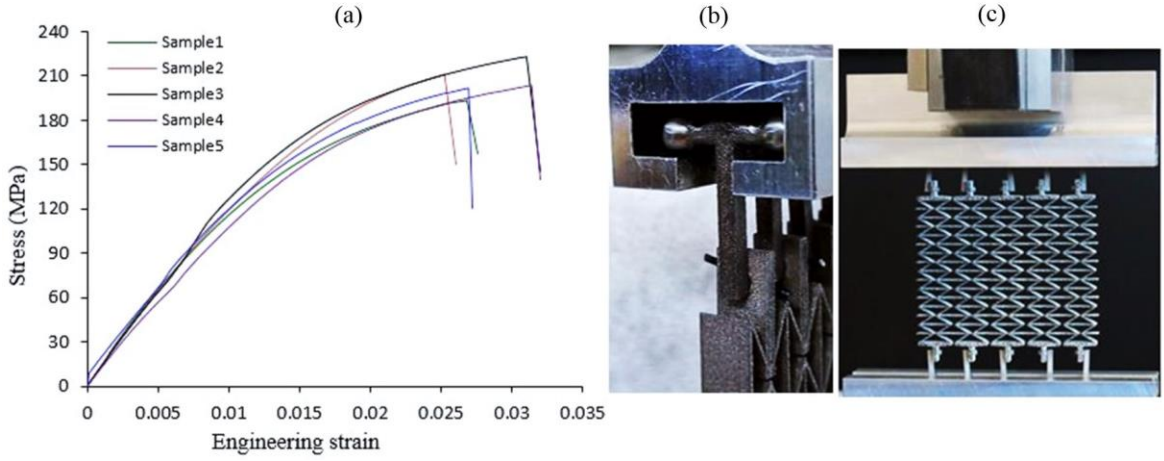

Figure 2. (a) Engineering stress-strain curves of the AlSi12 material, (b) Details of the fixtures holding one end of the sample, (c) Tensile test setup of a re-entrant honeycomb under X-loading.

3.2 Measurement of Poisson's ratio of re-entrant honeycomb and tensile stress

The history of Poisson's ratio of each sample was of primary interest in the current study. For the measurement of Poisson's ratio, a Digital VIC-2D Image Correlation System equipped with a 5-megapixel camera was used to capture the deformation images at one frame per second and calculate the axial and lateral strains of samples. Poisson's ratio, were calculated by the following formula**:**

$$\nu = -\varepsilon_L/\varepsilon_A \quad (1)$$

where, ν, ε_A and ε_L are Poisson's ratio, axial strain and lateral strain respectively.

4. Results and discussions

4.1 Tensile properties

Figure 3 (a) and (b) show the deformation of re-entrant honeycomb samples. In case of X-loading, the whole structure deforms by bending of incline struts figure 3 (a); while it deforms by bending and stretching of incline and vertical struts in case of Y-loading figure (b). The morphological figures also indicate that the failure of samples are catastrophic resulting from sudden fracture of incline walls. The experimental force-displacement curves of re-entrant honeycomb samples under both loading are shown in figure 3 (c). The force of the sample stretched in the X direction is lower than that loaded in the Y direction. Meanwhile, since the samples made of AlSi12 power does not display great plasticity, as indicated in figure 2(a), the auxetic honeycombs fracture at relatively small displacements (11.4 mm for X-loading and 4 mm for Y-loading). Therefore, the lack of plasticity causes the absence of plateau stage on the force-displacement curves of AlSi12 re-entrant honeycombs under loading in both axes. The comparisons imply that the loading direction plays a critical role in the tensile behaviour of the re-entrant honeycombs.

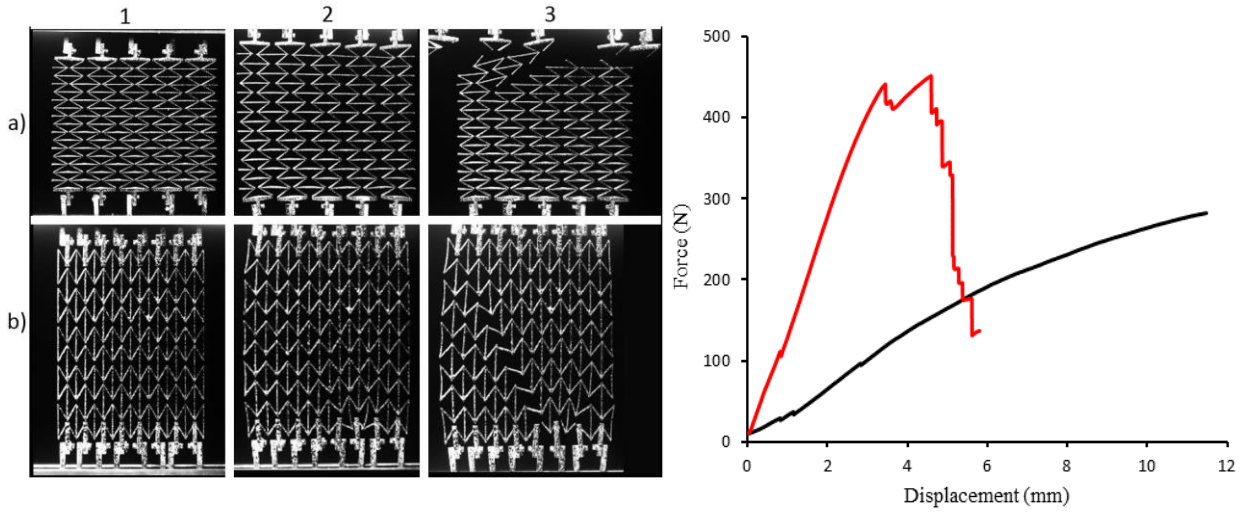

Figure 3. Deformation patterns of re-entrant honeycomb samples under (a) X-loading and (b) Y-loading (1- unreformed samples, 2- maximum displacement, 3- fracture), (c) Experimental force-displacement curves of re-entrant honeycomb samples.

4.2 Poisson's ratios

Digital Image Correlation (DIC) System was used to calculate the lateral and axial strains of the traced points of re-entrant honeycomb samples. Poisson's ratios were then calculated using Eq. (1) and plotted in figure 4. For both loading cases, Poisson's ratio of the re-entrant honeycomb remained negative. In the case of X-loading, the magnitude of Poisson's ratio increased monotonically. Conversely, in the case of Y-loading, the magnitude of Poisson's ratio decreased monotonically. Poisson's ratio of the re-entrant honeycombs is about 10 times as the former case. Under Y-loading, the Poisson's ratio of the re-entrant honeycomb varies from approximately -3.4 to -2.8 at the displacement of 0.7 mm and then remains almost constant till 2.6 mm (Figure 4b). Afterwards, a sudden decrease is observed, might be due to friction. Although lubricant was used, the lateral movement of the small fixtures was not fully free. This is required to be improved in the future tests.

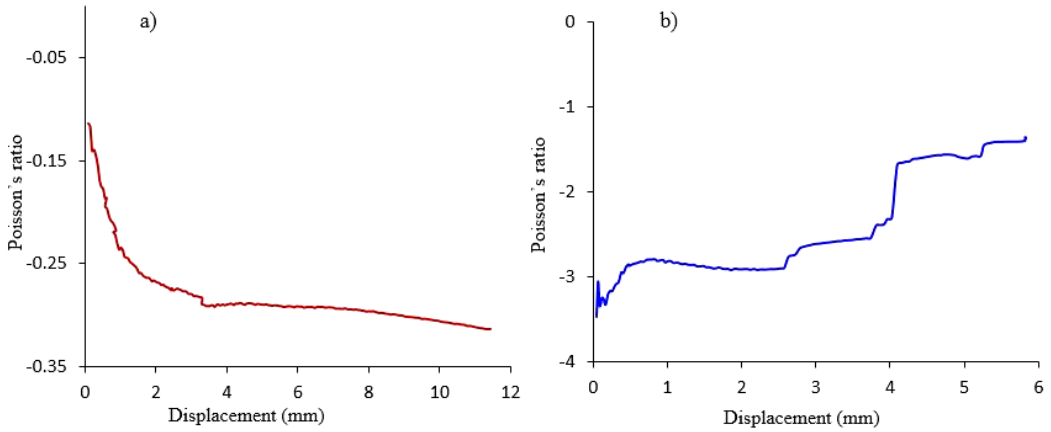

Figure 4. Experimental Poisson's ratios of re-entrant honeycomb under: (a) X-loading, (b) Y-loading.

5. Conclusions

AlSi12 powder was employed to manufacture two re-entrant honeycomb samples with identical geometrical parameters using SLM additive manufacturing technology. Standard tests were performed on dog-bone AlSi12 samples and results indicated the brittleness of this material. Quasi-static tensile tests were carried out on the auxetic honeycombs in the X and Y directions respectively. It was found that the loading direction has a considerable effect on the mechanical and auxetic behaviours of the re-entrant honeycombs. The auxetic samples fractured after a small displacement due to brittle cell wall material. The sample loaded in the Y direction withstood higher tensile force and underwent smaller deformation before fracture than that under X- direction. The magnitude of Poisson's ratios remained negative and increased (X-loading) or decreased (Y-loading) as further tension.

References

[1] Alderson A and Alderson K L 2007 Auxetic Materials *Proceedings of the Institution of* Mechanical Engineers Part G-Journal of Aerospace Engineering. **221(G4)** 565-575
[2] Strek T and Jopek H 2012 Effective mechanical properties of concentric cylindrical composites with auxetic phase *physica status solidi (b)* **249(7)** 1359-65
[3] Javadi A, Faramarzi A and Farmani R 2012 Design and optimization of microstructure of auxetic materials *Engineering Computations*, **29** 260-276.
[4] Lakes R and Elms K 1993 Indentability of Conventional and Negative Poisson's Ratio Foams *Journal of Composite Materials* **27** 1193-1202
[5] Alderson A 1999 A triumph of lateral thought *Chemistry & Industry* 384-391
[6] Wan H, Ohtaki H, Kotosaka S and Hu G 2004 A study of negative Poisson's ratios in auxetic honeycombs based on a large deflection model *European Journal of Mechanics - A/Solids* **23** 95-106
[7] Scarpa F 2008 Auxetic materials for bioprostheses [In the Spotlight] *IEEE Signal Processing Magazine* **25(5)** 128-126
[8] Muslija A and D áz Lantada A 2014 Deep reactive ion etching of auxetic structures: present capabilities and challenges *Smart Materials and Structures.* **23** 087001
[9] Lakes R 1987 Foam Structures with a Negative Poisson's Ratio Science **235**1038-40
[10] Yang, L 2011 Structural Design Optimization and Application of 3D Re-entrant Auxetic Structures *PhD Thesis, NC State Industrial Engineering Department*. Raleigh
[11] Li Y, Harrysson O, West H, Cormier D, 2012 Compressive properties of Ti-6Al-4V auxetic mesh structures made by electron beam melting, *Acta Mater*. **60 (8)** 3370–3379.
[12] Li S, Hassanin H, Attallah MM, Adkins NJE, Essa K 2016 The development of TiNi based negative Poisson's ratio structure using selective laser melting, *Acta Mater*. **105** 75–83.